

# Film thickness prediction in elastohydrodynamically lubricated elliptical contacts

A Canzi<sup>1</sup>, C H Venner<sup>2</sup>, and A A Lubrecht<sup>1\*</sup>

<sup>1</sup>LaMCoS, INSA-Lyon, CNRS UMR 5259, Université de Lyon, Villeurbanne, Lyon, France

<sup>2</sup>University of Twente, Enschede, The Netherlands

*The manuscript was received on 28 August 2009 and was accepted after revision for publication on 19 January 2010.*

DOI: 10.1243/13506501JET717

**Abstract:** This paper analyses the minimum and central film thickness evolution of elastohydrodynamically lubricated contacts, from circular to wide elliptical contacts. It is shown that already for moderate ellipticity, the minimum film thickness is found on the centre-line of the contact, rather than in the side lobes as for the circular contact. In such cases, the film thickness can be accurately predicted from an equivalent line contact, defined as the line contact with the same Hertzian pressure, radius of curvature, and speed and oil parameters. In this paper, a formula is presented to predict the central film thickness in elliptical contacts using prediction formulas for the line and circular contacts as limiting cases, and the results of numerical calculations to fit the film thickness variation with ellipticity. The formula gives an accurate prediction of the central film thickness over the entire ellipticity regime.

**Keywords:** elastohydrodynamically lubricated, elliptical contact line contact, film thickness prediction

## 1 INTRODUCTION

In order to reliably predict the performance of highly loaded lubricated contacts such as bearings and gears, contacts operating in the Elastohydrodynamically lubricated (EHL) regime have been studied for many years. Several researchers have presented predictive formulae for the film thickness in line and circular contacts based on simplified analyses for asymptotic cases and/or curve fits of numerical solutions [1, 2]. Also, for the more general case of wide elliptical contacts, such formulae have been presented [3–6]. However, a major problem is that these are either based on an extension of a circular contact formula or on curve-fitting of numerical results in a rather narrow range of load conditions and ellipticity values. As a result, neither of them can accurately predict the film thickness in the entire parameter regime ranging from the circular to the infinitely wide line contact. To derive such a formula is the objective of the research presented

in this paper. This work uses the function fit formulae presented by Moes for the circular and line contacts as starting point. Results of numerical simulations of the elliptical contact problem are used to study the film thickness variation with ellipticity going from circular to increasingly elliptical contacts. This variation is captured using a smooth transition function. In this way, an accurate predictive formula can be obtained. Its prediction tends for increasing ellipticity to the one-dimensional line contact solution, which is the physical limit of the wide elliptical contact.

The parameters used to describe the load and lubricant conditions are the Moes [7] dimensionless load parameter  $M$  and the dimensionless piezoviscosity parameter  $\bar{\alpha}$ .

First, the existing predictive formulae for line and circular contacts are reviewed and their predictions are compared with results of numerical calculations. Subsequently, the elliptical contact results are presented.

## 2 LINE CONTACT

The Moes dimensionless parameters for the line contact are

$$M_1 = \frac{W}{E'R_x} \left( \frac{\eta_0 u_\Sigma}{E'R_x} \right)^{-1/2} \quad (1)$$

\*Corresponding author: Laboratoire de Mécanique des Contacts, INSA de Lyon, UMR CNRS 5514 Ecole Centrale de Lyon, Batiment 113-20, 20 Avenue Albert Einstein, Villeurbanne, Lyon 69621, France.  
email: ton.lubrecht@insa-lyon.fr

$$L = \alpha E' \left( \frac{\eta_0 u_\Sigma}{E' R_x} \right)^{1/4} \quad (2)$$

$$\bar{\alpha} = \alpha p_h = L \sqrt{\frac{M_1}{2\pi}} \quad (3)$$

Moes [7] presented an equation for the dimensionless central film thickness using a function fit of four asymptotic solutions

$$H_c = [(H_{RI}^{7/3} + H_{EI}^{7/3})^{3s/7} + (H_{RP}^{-7/2} + H_{EP}^{-7/2})^{-2s/7}]^{1/s} \quad (4)$$

in which  $H$  is a dimensionless film thickness defined as

$$H = \frac{h}{R_x} \left( \frac{\eta_0 u_\Sigma}{E' R_x} \right)^{-1/2} \quad (5)$$

The four asymptotic solutions are as follows.  $H_{RI}$ : rigid isoviscous;  $H_{RP}$ : rigid piezoviscous;  $H_{EI}$ : elastic isoviscous solution;  $H_{EP}$ : elastic piezoviscous solution.

These asymptotic solutions were obtained from separate analyses of the particular problems

$$H_{RI} = 3M_1^{-1} \quad (6)$$

$$H_{RP} = 1.28666 L^{2/3} \quad (7)$$

$$H_{EI} = 2.62105 M_1^{-1/5} \quad (8)$$

$$H_{EP} = 1.31106 M_1^{-1/8} L^{3/4} \quad (9)$$

For example,  $H_{RI}$  can be obtained analytically from the solution of the rigid-isoviscous problem,  $H_{EI}$  from the Herrebrugh [8] elastic isoviscous solution,  $H_{EP}$  from the Ertel [9] solution.

The function  $s$  ensures a smooth transition between the different regimes

$$s = \frac{1}{5} \left[ 7 + 8 \exp\left(-2 \frac{H_{EI}}{H_{RI}}\right) \right] \quad (10)$$

The constants in this function were determined by optimal curve fit comparing the results with the values obtained from numerical solutions.

The equation was developed assuming an incompressible lubricant. Predictions for the case of a compressible lubricant can be obtained, to a good approximation, easily using the fact that

$$H_{Ccomp} = \frac{H_{Cincomp}}{\bar{\rho}(p_h)} \quad (11)$$

which is a direct consequence of the shear flow dominance in the high viscosity/small film thickness central region [5].

### 3 CIRCULAR CONTACT

The Moes dimensionless load parameters  $M_2$  and the Moes dimensionless material parameter  $L$  for the

circular contact are

$$M_2 = \frac{F}{E' R_x^2} \left( \frac{\eta_0 u_\Sigma}{E' R_x} \right)^{-3/4} \quad (12)$$

$$L = \alpha E' \left( \frac{\eta_0 u_\Sigma}{E' R_x} \right)^{1/4} \quad (13)$$

and the piezoviscous parameter is related according to

$$\bar{\alpha} = \alpha p_h = \frac{L}{\pi} \sqrt{\frac{3M_2}{2}} \quad (14)$$

In the same way as for a line contact, Moes [7] derived a central film thickness function fit for the circular contact. This fit is based on particular solutions for the asymptotic regimes and numerical simulation results of the complete circular problem. However, for the two-dimensional case, the asymptotic solutions could not be derived analytically. They were obtained numerically by solving the simplified problems for the case of rigid isoviscous and elastic isoviscous [10]. The formula appears in the literature in several slightly different variations. In this paper, the version presented in reference [10] is used

$$H_c = \{[(1.70tM_2^{-1/9}L^{3/4})^r + (1.96M_2^{-1/9})^r]^{s/r} + (47.3M_2^{-2})^s\}^{t/s} \quad (15)$$

with

$$r = \exp\left(1 - \frac{6}{L+8}\right) \quad (16)$$

$$s = 12 - 10 \exp(-M_2^{-2}) \quad (17)$$

$$t = 1 - \exp\left(-\frac{0.9M_2^{1/6}}{L^{1/6}}\right) \quad (18)$$

The functions  $r$ ,  $s$ , and  $t$  create a smooth transition between the asymptotic solutions. The constants appearing in these functions were determined using results of numerical solutions of the circular contact problem for a wide range of conditions.

As for the line contact case, the formula is restricted to an incompressible lubricant. However, as explained above, the prediction can easily be corrected accounting for the central film thickness reduction due to compressibility.

### 4 ELLIPTICAL CONTACT

The ellipticity  $D$  of the contact is defined by the ratio  $D = R_x/R_y$ . Note that this is the inverse of the classical way to define ellipticity. According to Nijenbanning *et al.* [4], the Moes dimensionless parameters for the elliptical problem are  $M_2$  and  $L$ , as defined for the circular contact, and  $D$ . The piezoviscous parameter is

related according to

$$\bar{\alpha} = \alpha p_h = \frac{L}{\pi} \left( \frac{3M_2\kappa}{2} \right)^{1/3} \left( \frac{(1+D)\pi}{4E_c} \right)^{2/3} \quad (19)$$

The elliptical contact problem was studied extensively analytically and numerically (i.e. by Chittenden *et al.* [5], Hamrock and Dowson [3], Hooke [6, 11, 12], Evans and Snidle [13], and Nijenbanning *et al.* [4], and film thickness formulae were presented). Most papers consider the so-called wide elliptical contacts in which the axis of the Hertzian contact ellipse in the direction of the flow is smaller than in the cross-flow direction. Nijenbanning *et al.* [4] presented a formula for the central film thickness using the circular contact central film thickness formula derived by Moes as a basis. The disadvantage of the presented formulae is the limited validity in terms of the ellipticity ratio as the physical limit of an infinitely wide contact is not incorporated. A formula which does incorporate this limit can be obtained using the definition of an equivalent line contact.

## 5 EQUIVALENT LINE CONTACT

For an elliptical contact, the equivalent line contact is defined as the infinitely wide line contact problem for which the values of the 1D dimensionless Moes parameters are such that the contact has the same radius of curvature in the direction of the flow, the same Hertzian pressure, and the same rolling velocity and viscosity. For an elliptical contact with a given  $M_2$  and  $L$ , the parameters characterizing the 1D equivalent line contact are

$$L = L \quad (20)$$

$$M_1 = \frac{2}{\pi} (1.5M_2\kappa)^{2/3} \left( \frac{(1+D)\pi}{4E_c} \right)^{4/3} \quad (21)$$

The piezoviscous parameter is related according to [4]

$$\bar{\alpha} = \alpha p_h = L \sqrt{\frac{M_1}{2\pi}} \quad (22)$$

## 6 NUMERICAL SOLUTION

The governing equations (Reynolds, film thickness, and force balance) were discretized on a uniform grid using second-order accurate discretization. In the numerical calculations, the viscosity pressure relation used is the Roelands [14] equation and the effect of compressibility is taken into account through the Dowson and Higginson [1] relation. Multilevel methods were used to solve the discrete equations and for

**Table 1** Computed Moes 2D central and minimum film thickness as a function of the mesh size on the grid for  $\bar{\alpha} = 10$ ,  $M_2 = 2027$ ,  $D = 0.2$  (compressible lubricant)

Grid	$H_c$	$H_m$
$128 \times 128$	1.365	0.926
$256 \times 256$	1.760	1.393
$512 \times 512$	1.856	1.517
$1024 \times 1024$	1.880	1.549
$2048 \times 2048$	1.886	1.556

the fast evaluation of the elastic deformation integrals. For details, the reader is referred to reference [15]. As an example of the accuracy of the results, Table 1 shows the minimum and central film thickness as a function of the mesh size for the elliptical contact with parameters  $\bar{\alpha} = 10$ ,  $M_2 = 2027$ ,  $D = 0.2$ . These results are typical for the accuracy of the computations (i.e. film thickness values are accurate to an error less than 1 per cent).

## 7 RESULTS

First, the two extreme cases are considered (i.e. the 1D line contact problem and the circular contact problem as these two formulae are the core of the formula to be derived).

Table 2 presents results of numerical simulations for the line contact problem and values predicted by the Moes line contact central film thickness formula corrected for compressibility. The values of  $M_1$  and  $\bar{\alpha}$  are such that the operating conditions cover the entire range from nearly isoviscous to piezoviscous. The results show that the Moes formula is accurate over the entire EHL range. The difference between the prediction and the numerical calculation is less than 10 per cent in every calculated case.

Results for the circular contact case are presented in Table 3: the predicted central film thickness values according to the Moes formula for the circular contact, corrected for the effect of compressibility, and the results of numerical simulations, for a range of conditions.

**Table 2** Moes 1D compressible line contact curve fits versus calculation

$\bar{\alpha}$	$M_1$	$H_c$ Moes formula	$H_c$ calculated
20	17.97	4.77	4.91
20	52.55	2.98	2.90
10	17.97	3.20	3.13
10	52.55	2.06	1.93
5	17.97	2.30	2.20
5	52.55	1.54	1.46

**Table 3** Moes 2D film thickness predictions and calculated values (compressible lubricant)

$\bar{\alpha}$	$M_2$	$H_c$ Moes formula	$H_c$ calculated
20	100	4.05	4.30
20	500	2.64	2.64
10	100	2.73	2.73
10	500	1.84	1.73
5	100	1.99	1.86
5	500	1.39	1.27

The results presented in Table 3 show that over the entire range of parameters considered, the Moes formula predicts the dimensionless central film thickness accurately up to an error of 10 per cent.

Having determined the accuracy of the two extreme cases for wide elliptical contacts (i.e. the infinitely wide and the circular contact, the variation of the film thickness with varying ellipticity is studied next). To show the asymptotic trend to the infinitely wide line contact, it is crucial that the results are presented in terms of a dimensionless parameter that does not depend on the deformation and the ellipticity itself. The simplest parameter satisfying this requirement is the Hamrock–Dowson dimensionless film thickness parameter:  $H = h/R_x$ .

To observe the asymptotic behaviour of the film thickness with increasing ellipticity, the dimensionless material parameter  $L$  and  $\bar{\alpha}$  are kept constant. Hence, for each value of  $D$ , the Moes dimensionless load parameter is recalculated. If  $M_{2c}$  is the value of  $M_2$  for  $D = 1$  and for given values of  $L$  and  $\bar{\alpha}$ , then

$$M_2 = \frac{M_{2c}}{\kappa} \left[ \frac{4E_c}{(1 + D)\pi} \right]^2 \tag{23}$$

Hence, the operating conditions are defined by  $M_{2c}$  and  $\bar{\alpha}$ .

In Figs 1 and 2, the centre-line film thickness profiles  $h/R_x(x/a_x)$  are shown for the cases  $\bar{\alpha} = 0$ ,  $M_2 = 100$ , and  $\bar{\alpha} = 10$ ,  $M_2 = 100$ , with  $D \in [0.01, 1]$  as well as the equivalent line contact solution. It can clearly be seen that for wide ellipses  $D < 0.05$ , the elliptical central film thickness perfectly fits the equivalent line contact in both the inlet, the high-pressure zone, and at the outlet. Thus the equivalent line contact represents a good approximation for the wide elliptical contact.

Figure 3 illustrates the shape of the numerical film thickness solution on the entire domain by means of contour plots. In the figure are shown  $h/R_x(x/a_x, y/a_y)$  for the case  $\bar{\alpha} = 2$  and  $M_{2c} = 100$ , and  $D = 1.0-0.01$ . It is recalled that the Hertzian pressure for each of the contacts is the same. It can be seen that with increasing ellipticity, the film shape near the side of the contact (i.e. in the side lobes, changes considerably). The circular contact exhibits the characteristic features of a flat central region and a minimum film thickness occurring in the side lobes. With increasing ellipticity, the

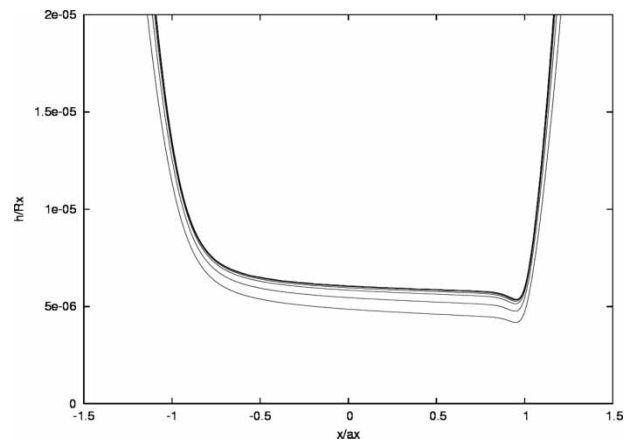


**Fig. 1** Centre-line film thickness as a function of  $x/a_x$  for  $D = 1.0, 0.5, 0.2, 0.1, 0.05, 0.02, 0.01$  and equivalent line contact (bottom to top;  $\bar{\alpha} = 0$ ,  $M_{2c} = 100$ )

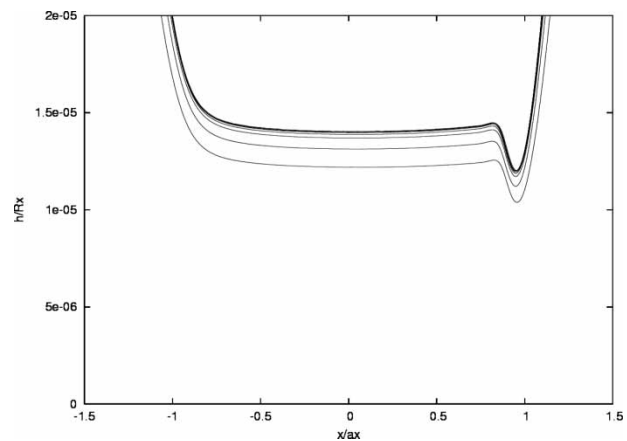


**Fig. 2** Centre-line film thickness as a function of  $x/a_x$  for  $D = 1.0, 0.5, 0.2, 0.1, 0.05, 0.02, 0.01$  and equivalent line contact (bottom to top;  $\bar{\alpha} = 10$ ,  $M_{2c} = 100$ )

film thickness in the central region increases to the equivalent line contact value. However, at the same time the film thickness in the side lobes increases even more. For values of  $D < 0.2$ , the minimum film thickness no longer occurs in the side lobes but on the centre-line as is the case for the infinitely wide line contact. This is further illustrated in Figs 4 and 5 for two other loading cases and different values of  $D$ . In the figure, details of the film profile in the direction of the flow and perpendicular to the flow are shown. Note that in the figure  $h/R_x(x/a_x, y/a_y = 0)$  for  $x/a_x > 0$  and  $H(x/a_x = 0, y/a_y)$  for  $(y/a_y < 0)$  are combined. The different behaviour of the film thickness in the central region and near the side lobes can be attributed to the compressibility [16]. As the pressure in the side lobe region is very low compared with the pressure in the centre of the contact, the compressibility affects the film thickness in the centre but not in the side lobes.

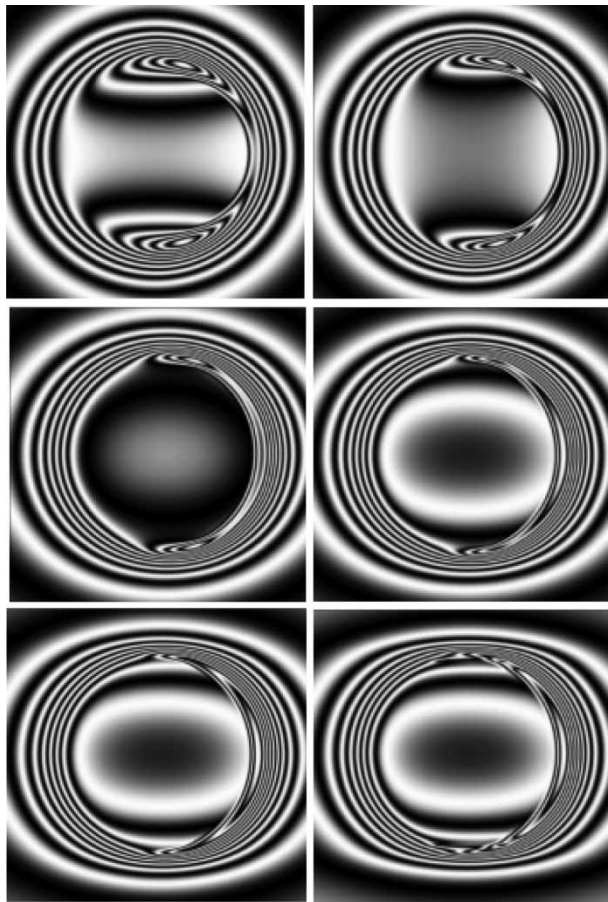


**Fig. 3** Elliptical contact film thickness distribution for  $D = 1.0, 0.5, 0.2, 0.1, 0.05, 0.01$  (top left to bottom right) for the case ( $\bar{\alpha} = 2$  and  $M_{2c} = 100$ )

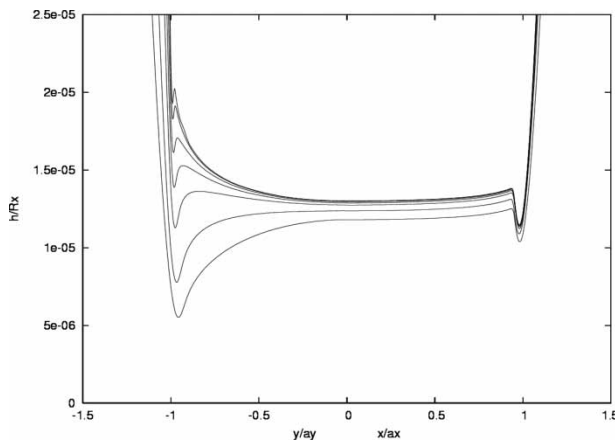


**Fig. 4** Film thickness as a function of  $x/a_x$  and  $y/a_y$  for  $D = 1.0, 0.5, 0.2, 0.1, 0.05, 0.02, 0.01$  (bottom to top;  $\bar{\alpha} = 20$  and  $M_{2c} = 500$ )

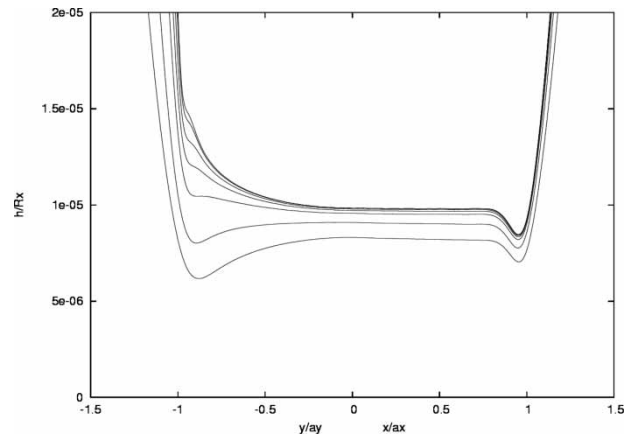


**Fig. 5** Film thickness as a function of  $x/a_x$  and  $y/a_y$  for  $D = 1.0, 0.5, 0.2, 0.1, 0.05, 0.02, 0.01$  (bottom to top;  $\bar{\alpha} = 5$  and  $M_{2c} = 100$ )

**Table 4** Evolution of  $H_c$  and  $H_m$  with ellipticity for  $\bar{\alpha} = 20$  and  $M_{2c} = 500$

$D$	1	0.5	0.2	0.1	0.05	0.01
$H_c$	2.64	2.77	2.85	2.88	2.90	2.91
$H_m$	1.27	1.47	2.11	2.54	2.55	2.56
$H_c/H_m$	2.08	1.88	1.35	1.13	1.14	1.14

**Table 5** Evolution of  $H_c$  and  $H_m$  with ellipticity for  $\bar{\alpha} = 10$  and  $M_{2c} = 100$

$D$	1	0.5	0.2	0.1	0.05	0.01
$H_c$	2.73	2.94	3.06	3.10	3.12	3.14
$H_m$	1.50	1.93	2.50	2.66	2.67	2.69
$H_c/H_m$	1.82	1.52	1.22	1.17	1.17	1.17

From Figs 4 and 5 and Tables 3 and 4, it can be observed that the increase of the central film thickness with increasing ellipticity to the equivalent line contact value is monotonous. This is shown in detail in Fig. 6 where the calculated central and minimum film thickness are shown as a function of  $D$ . Also shown are the predicted minimum and central film thicknesses according to the Hamrock–Dowson formula.

Figure 6 shows that the Hamrock–Dowson prediction decreases for low values of  $D$ . This decrease is not physical. The Hooke prediction suffers from a similar problem.

The curve fit chosen in this paper does not use an exponential function as Hamrock and Dowson [3], Chittenden *et al.* [5], Hooke [6] or Nijenbanning *et al.* [4] but a trigonometric function which blends the circular and line contact prediction. This solution uses the Moes 2D circular central film thickness prediction, the Moes 1D line prediction, and fits the numerical calculations for intermediate ellipticities  $D$ . The new formula is expected to have a good precision for wide ellipses, because it uses the 1D equivalent line contact which, after all, is the solution for infinitely wide ellipses. The following incompressible central

Finally, Tables 4 and 5 quantitatively illustrate these changes in central and minimum film thickness with increasing ellipticity.

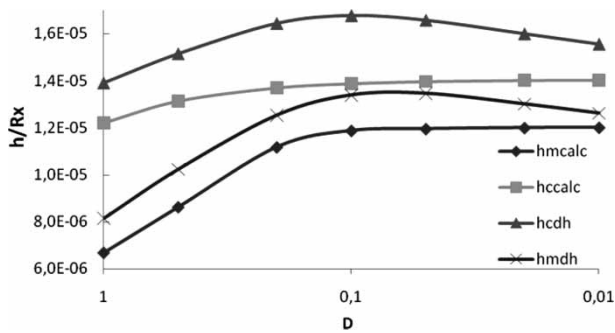


**Fig. 6** Hamrock Dowson minimum, central film thickness prediction, and calculated minimum and central film thickness versus  $D$  ( $\bar{\alpha} = 10$  and  $M_{2c} = 100$ )

film thickness prediction function is proposed

$$H_{Cincomp} = H_{C2D} + \frac{2(H_{C1D} - H_{C2D})}{\pi} a \tan\left(\frac{1}{D-1}\right) \quad (24)$$

where  $H_{C1D}$  is the Moes equivalent line contact prediction and  $H_{C2D}$  the Moes circular contact prediction.

The compressible central film thickness prediction can subsequently be obtained as described before by dividing this value by the relative central density. This value is well approximated by the relative density at the maximum Hertzian pressure.

Tables 4 and 5 show the evolution of the central film thickness and of the minimum film thickness for increasing ellipticity.

The accuracy of this new formula is illustrated by the results presented in Table 6. For a wide range of conditions, the calculated and predicted values are shown. The difference between the predicted values and the calculated values is below 10 per cent for every case. This difference is essentially due to the precision of the Moes circular and line prediction. The only complication in the use of the formula is the calculation of the equivalent line contact parameters. However, this can easily be implemented in a small computer program [17].

## 8 DISCUSSION

In this work, the authors have decided to sidestep the difficult prediction of the minimum film thickness in the side lobes [6, 11, 12]. As indicated in reference [15] and illustrated in Figs 4 to 6, the minimum side lobe value quickly exceeds the compressible central film thickness as ellipticity increases. The side lobe value becomes a local minimum, with limited implications on contact performance. Hence the choice of a compressible film prediction avoids this problem. For those preferring another compressibility equation,

**Table 6** Predicted versus calculated film thickness for different operating conditions

$\bar{\alpha} = 10$ and $M_{2c} = 100$						
$D$	1	0.5	0.2	0.1	0.05	0.01
$H_c$ (CELINE)	2.73	2.97	3.13	3.17	3.19	3.20
$H_{Ccalc}$	2.73	2.94	3.06	3.10	3.12	3.14
$\bar{\alpha} = 20$ and $M_{2c} = 500$						
$D$	1	0.5	0.2	0.1	0.05	0.01
$H_c$ (CELINE)	2.64	2.81	2.93	2.96	2.97	2.98
$H_{Ccalc}$	2.64	2.77	2.85	2.88	2.90	2.91
$\bar{\alpha} = 5$ and $M_{2c} = 100$						
$D$	1	0.5	0.2	0.1	0.05	0.01
$H_c$ (CELINE)	1.99	2.14	2.25	2.27	2.29	2.29
$H_{Ccalc}$	1.86	2.03	2.14	2.17	2.19	2.20
$\bar{\alpha} = 10$ and $M_{2c} = 500$						
$D$	1	0.5	0.2	0.1	0.05	0.01
$H_c$ (CELINE)	1.84	1.95	2.03	2.05	2.05	2.06
$H_{Ccalc}$	1.73	1.82	1.89	1.91	1.92	1.93
$\bar{\alpha} = 0$ and $M_{2c} = 100$						
$D$	1	0.5	0.2	0.1	0.05	0.01
$H_c$ (CELINE)	0.98	1.11	1.19	1.21	1.22	1.23
$H_{Ccalc}$	1.09	1.22	1.31	1.33	1.34	1.35

a quick recalculation of the compressibility at the Hertzian pressure allows a correction of the central film thickness value.

## 9 CONCLUSION

The Hamrock–Dowson, Nijenbanning, or Chittenden predictions provide accurate film thickness approximations for moderately wide elliptical contacts. However, these predictions are no longer accurate for very wide contacts. The method presented in this work and implemented in CELINE [17] uses an equivalent line contact to overcome this problem. The formula is based on the Moes circular and line contact predictions. The difference between calculated and predicted values is less than 10 per cent for all ellipticities and operating conditions.

© Authors 2010

## REFERENCES

- Dowson, D.** and **Higginson, G. R.** *Elasto-hydrodynamic lubrication: the fundamentals of roller and gears lubrication*, 1966 (Pergamon Press, Oxford).
- Hamrock, B. J.** and **Dowson, D.** Isothermal elastohydrodynamic lubrication of point contacts. Part 1. Theoretical formulation. *ASME JOT*, 1976, **98**, 223–229.
- Hamrock, B. J.** and **Dowson, D.** Isothermal elastohydrodynamic lubrication of point contacts. Part 2. Ellipticity parameter results. *ASME JOT*, 1976, **98**, 375–383.
- Nijenbanning, G., Venner, C. H.,** and **Moes, M.** Film thickness in elastohydrodynamically lubricated elliptic contacts. *Wear*, 1994, **176**, 217–229.

- 5 Chittenden, R. J., Dowson, D., Dunn, J. F., and Taylor, C. M.** A theoretical analysis of the isothermal elastohydrodynamic lubrication of concentrated contacts. I. Direction of lubricant entrainment coincident with the major axis of the contact ellipse. *Proc. R. Soc. London*, 1985, **A397**, 345–369.
- 6 Hooke, C. J.** Minimum film thicknesses in lubricated point contacts operating in the elastic piezoviscous regime. *Proc. IMechE, Part C: J. Mechanical Engineering Science*, 1988, **202**, 73–83. DOI: 10.1243/PIME\_PROC\_1988\_202\_092\_02.
- 7 Moes, H.** *Lubrication and beyond*, 2000, available from <http://www.tr.ctw.utwente.nl/Research/Publications/Books%20%26%20Chapters/book%202000b.doc/index.html>.
- 8 Herrebrugh, K.** Solving the incompressible and isothermal problem in elastohydrodynamics through an integral equation. *ASME JOT*, 1968, **90**, 262–270.
- 9 Ertel, A. M.** Hydrodynamic lubrication based on new principles. *Akad. Nauk SSSR Prikadnaya Matematika Mekhanika*, 1939, **3**(2), 41–52.
- 10 Venner, C. H.** Multilevel solution of the EHL line and point contact problems, 1991, available from <http://www.tr.ctw.utwente.nl/Research/Publications/index.html>.
- 11 Hooke, C. J.** The influence of piezo-viscosity on the minimum film thickness in heavily loaded contacts. *Proc. IMechE, Part C: J. Mechanical Engineering Science*, 1990, **204**, 117–125. DOI: 10.1243/PIME\_PROC\_1990\_204\_085\_02.
- 12 Hooke, C. J.** An interpolation procedure for the minimum film thickness in point contacts. *Proc. IMechE, Part C: J. Mechanical Engineering Science*, 1990, **204**, 199–206. DOI: 10.1243/PIME\_PROC\_1990\_204\_095\_02.
- 13 Evans, H. P. and Snidle, R. W.** Analysis of elastohydrodynamic lubrication of elliptical contacts with rolling along the major axis. *Proc. Instn Mech. Engrs, Part C: J. Mechanical Engineering Science*, 1983, **197**, 209–211. DOI: 10.1243/PIME\_PROC\_1983\_197\_098\_02.
- 14 Roelands, C. J. A.** *Correlational aspects of the viscosity-temperature-pressure relationship of lubricating oils*. PhD Thesis, Technische Hogeschool Delft, The Netherlands.
- 15 Venner, C. H. and Lubrecht, A. A.** *Multilevel methods in lubrication*, vol. 37, 2000, Tribology Series (Elsevier).
- 16 Lubrecht, A. A., Venner, C. H., and Colin, F.** Film thickness calculation in elasto-hydrodynamic lubricant line and elliptical contacts; the Dowson, Higginson, Hamrock contribution. *Proc. IMechE, Part J: J. Engineering Tribology*, 2009, **223**(J3), 511–515. DOI: 10.1243/13506501JET508.
- 17 CELINE.** Computer program calculating the elliptical central film thickness, freeware, available from the LaMCoS website, INSA-Lyon.

## APPENDIX

## Notation

$a_x$	half-width of Hertzian contact in $x$ -direction (= $6R_x F \kappa E_c / [E' \pi (1 + D)]^{1/3}$ )
$a_y$	half-width of Hertzian contact in $y$ -direction (= $a_x / \kappa$ )
$D$	ratio of reduced radii of curvature (= $R_x / R_y$ )
$E'$	reduced modulus of elasticity (Pa) ( $2/E' = (1 - \nu_1^2)/E_1 + (1 - \nu_2^2)/E_2$ )
$E_c$	elliptic integral $E_c(\kappa) = \int_0^{2\pi} d\phi / \sqrt{(\cos^2 \phi + \kappa^2 \sin^2 \phi)}$
$F$	2D load (N)
$h$	film thickness (m)
$H$	dimensionless film thickness (Moes; = $h/R_x (E'R_x/\eta_0 u_\Sigma)^{1/2}$ )
$L$	dimensionless material parameter (Moes; = $\alpha E' (\eta_0 u_\Sigma / E'R_x)^{1/4}$ )
$M_1$	1D dimensionless load parameter (Moes; = $(w_1/E'R_x)(\eta_0 u_\Sigma / E'R_x)^{-1/2}$ )
$M_2$	2D dimensionless load parameter (Moes; = $(F/E'R_x^2)(\eta_0 u_\Sigma / E'R_x)^{-3/4}$ )
$p$	pressure (Pa)
$p_h$	maximum Hertzian pressure (Pa)
$R_x$	reduced radius of curvature in $x$ -direction (m) ( $1/R_x = 1/R_{x1} + 1/R_{x2}$ )
$R_y$	reduced radius of curvature in $y$ -direction (m) ( $1/R_y = 1/R_{y1} + 1/R_{y2}$ )
$u_\Sigma$	sum velocity (m/s) ( $u_\Sigma = u_1 + u_2$ )
$u_1$	velocity of the lower surface (m/s)
$u_2$	velocity of the upper surface (m/s)
$w_1$	1D load per unit length (N/m)
$\alpha$	pressure viscosity index (Pa)
$\tilde{\alpha}$	dimensionless parameter (= $\alpha p_h$ )
$\eta_0$	viscosity at ambient pressure (Pa s)
$\kappa$	ellipticity ratio (= $a_x/a_y$ )
$\nu$	Poisson ratio
$\rho$	density (kg/m <sup>3</sup> )
$\bar{\rho}$	relative density (–) ( $\bar{\rho}(p) = \rho(p)/\rho_0$ )